Detecting a New Source for Photochemically Induced Dynamic Nuclear Polarization in the LOV2 Domain of Phototropin by Magnetic-Field Dependent C-13 NMR Spectroscopy

ARTICLE *in* THE JOURNAL OF PHYSICAL CHEMISTRY B · SEPTEMBER 2014

Impact Factor: 3.3 · DOI: 10.1021/jp507134y · Source: PubMed

THE JOURNAL OF PHYSICAL CHEMISTRY B

Article

pubs.acs.org/JPCB

Detecting a New Source for Photochemically Induced Dynamic Nuclear Polarization in the LOV2 Domain of Phototropin by Magnetic-Field Dependent ^{13}C NMR Spectroscopy

Gerd Kothe,*[,†] Michail Lukaschek,[†] Gerhard Link,[†] Sylwia Kacprzak,[†] Boris Illarionov,[‡] Markus Fischer,[‡] Wolfgang Eisenreich,[§] Adelbert Bacher,[§] and Stefan Weber*[,†]

[†]Institut für Physikalische Chemie, Albert-Ludwigs-Universität Freiburg, Albertstr. 21, 79104 Freiburg, Germany

[‡]Institut für Lebensmittelchemie, Universität Hamburg, Bundesstr. 45, 20146 Hamburg, Germany

[§]Lehrstuhl für Biochemie, Technische Universität München, Lichtenbergstr. 4, 85748 Garching, Germany

Supporting Information

ABSTRACT: Phototropin is a flavin mononucleotide (FMN) containing blue-light receptor, which regulates, governed by its two LOV domains, the phototropic response of higher plants. Upon photoexcitation, the FMN cofactor triplet state, ^{3}F, reacts with a nearby cysteine to form a covalent adduct. Cysteine-to-alanine mutants of LOV domains instead generate a flavin radical upon illumination. Here, we explore the formation of photochemically induced dynamic nuclear polarization (CIDNP) in LOV2-C450A of *Avena sativa* phototropin and demonstrate that photo-CIDNP observed in solution ^{13}C NMR spectra can reliably be interpreted in terms of solid-state mechanisms including a novel triplet mechanism. To minimize cross-polarization, which transfers light-induced magnetization to adjacent ^{13}C nuclei, our experiments were performed on proteins reconstituted with specifically ^{13}C-labeled flavins. Two potential sources for photo-CIDNP can be identified: The photogenerated triplet state, ^{3}F, and the triplet radical pair $^3(F^{-\bullet}W^{+\bullet})$, formed by electron abstraction of ^{3}F from tryptophan W491. To separate the two contributions, photo-CIDNP studies were performed at four different magnetic fields ranging from 4.7 to 11.8 T. Analysis revealed that, at fields <9 T, both $^3(F^{-\bullet}W^{+\bullet})$ and ^{3}F contribute to photo-CIDNP, whereas at high magnetic fields, the calculated enhancement factors of ^{3}F agree favorably with their experimental counterparts. Thus, we have for the first time detected that a triplet state is the major source for photo-CIDNP in a photoactive protein. Since triplet states are frequently encountered upon photoexcitation of flavoproteins, the novel triplet mechanism opens up new means of studying electronic structures of the active cofactors in these proteins at atomic resolution.

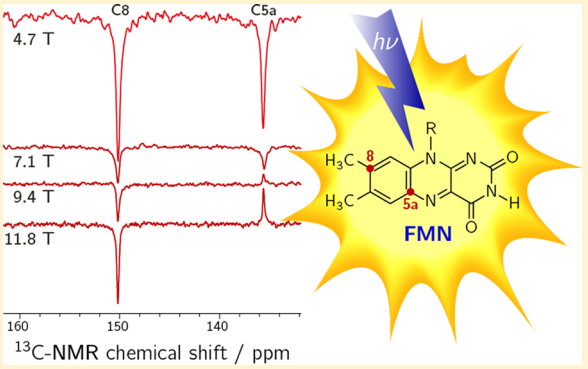

INTRODUCTION

In 1978, Kaptein et al. demonstrated that chemically induced dynamic nuclear polarization (CIDNP), generated in photochemical reactions between an excited dye and certain amino acid side chains on the surface of a protein, could be used to monitor the exposure of these residues.[1] In the period following, this liquid-state photo-CIDNP method proved a powerful probe of protein surface structure and protein folding.[2,3] The discovery that photo-CIDNP in photoactive proteins builds up under solid-state conditions opened a new area for application of the technique.[4] Using ^{15}N and ^{13}C magic-angle spinning NMR, photo-CIDNP effects were detected in practically all bacterial and plant photosynthetic reaction centers.[5−8] From an analysis of the observed photo-CIDNP spectra employing three solid-state radical pair mechanisms, i.e., three-spin mixing (TSM),[9−11] differential decay (DD),[12] and differential relaxation (DR),[13,14] detailed information was obtained on the electronic structure of the active cofactors at atomic resolution.[15]

Recently, photo-CIDNP was also observed in nonphotosynthetic systems, namely the LOV (light, oxygen, and voltage) domains of phototropin, by both solution[16−18] and solid-state[19,20] ^{13}C NMR spectroscopy. Phototropin is a flavin mononucleotide (FMN) containing blue-light receptor, which regulates, governed by its two LOV domains, the phototropic response of higher plants.[21−24] Upon photoexcitation, the triplet state of the flavin chromophore, ^{3}FMN ≡ ^{3}F, reacts with a nearby cysteine to form a covalent adduct.[25−27] Cysteine-to-alanine mutants of the LOV domains are unable to form that adduct but generate an FMN radical upon illumination.[16,17,28,29] In this contribution, we explore the magnetic-

Received: July 17, 2014
Revised: September 10, 2014
Published: September 10, 2014

   dx.doi.org/10.1021/jp507134y | J. Phys. Chem. B 2014, 118, 11622−11632

field dependent formation of photo-CIDNP in the LOV2-C450A mutant of *Avena sativa* phototropin, reconstituted with ^{13}C-labeled FMN. Generally, solution ^{13}C NMR spectra of the LOV2 mutant are recorded both in the dark and under blue-light irradiation, and the stationary enhancement factors $\varepsilon^{exp}(i)$ of the various ^{13}C nuclei i are analyzed using different solid-state photo-CIDNP mechanisms. Particular emphasis is given to the role of a novel triplet mechanism.[30] Study reveals that at higher magnetic fields ^{3}F is the major photo-CIDNP source in the blue-light receptor phototropin.

MATERIALS AND METHODS

Materials. [U-$^{13}C_{17}$]Riboflavin was prepared by fermentation of a riboflavin-producing *Bacillus subtilis* strain using [U-$^{13}C_6$]glucose as carbon source.[31] Other ^{13}C-labeled riboflavin isotopologs were prepared by chemical or enzyme-assisted syntheses.[31−34]

The preparation of the recombinant LOV2-C450A domain (amino acid residues 405 to 559) of *Avena sativa* phototropin and the reconstitution with isotope-labeled FMN follows procedures that have been reported elsewhere.[27]

NMR Spectroscopy. ^{13}C NMR spectra were measured at 278 K using standard Bruker NMR instrumentation at four different magnetic fields involving B_0 = 5.874 T (4.699 T), B_0 = 7.049 T, B_0 = 9.398 T, and B_0 = 11.747 T. At each field, spectra were recorded both in the dark and under blue light irradiation using a 5 mm ^{1}H/^{13}C solution probe. A nonselective $\pi/2$ pulse and composite pulse proton decoupling were used in all photo-CIDNP experiments. The recycle delay was 4 s. Free-induction decays (FIDs) were processed using exponential multiplication.

Blue-light irradiation was carried out with a continuous-wave diode laser (DHOM-445-600) at a wavelength of 445 nm and a laser power of 600 mW. Excitation of the sample in the NMR probe was achieved with a home-built fiber optic device. To minimize photostress on the sample, the light spectra were taken with only 64 scans. For the dark spectra 10 000−19 000 FIDs were accumulated to improve the signal-to-noise ratio.

DFT Computations. Two different molecular models of FMN have been considered: (i) isolated FMN and (ii) FMN in the binding site of the LOV2 domain of *Avena sativa* phototropin. The molecular structure of the isolated FMN, for simplicity, has been modeled by lumiflavin, in which the ribityl monophosphate side chain was replaced by a methyl group. Geometry optimization of the lowest triplet state was then carried out at the time-dependent density functional (TD-DFT) level,[35−37] using the gradient-corrected BP86 functional[38,39] and def2-TZVP Gaussian-type-orbital basis sets.[40] Def2-TZVP auxiliary basis sets[41] were used to fit the electron density (RI-DFT approximation).[42−44] Geometry optimization calculations were performed with the TURBOMOLE program.[45]

The model of FMN in the binding site of the LOV2 domain of *Avena sativa* phototropin is based on the 1.40-Å resolution X-ray structure obtained for the frozen protein in the dark.[46] In this structure, five residues, Q513, N492, N482, Q454, and N449, have been identified to interact strongly with FMN. In our model, the ribityl monophosphate side chain was cut after carbon C5′ and terminated by a hydrogen atom; all five amino acid residues were substituted by *N*-methylformamide molecules. We kept the intermolecular structure parameters as well as the structure of the truncated ribityl side chain at their crystallographic values.[46] However, all other intramolecular parameters as well as the positions of all hydrogen atoms were fully optimized. To conveniently take into account all required constraints, geometry optimization was carried out using the ORCA program package[47] and its fragment optimization option. The optimization has been carried out for a singlet ground state at the gradient-corrected (BP86 functional[38,39]) DFT level employing def2-TZVP Gaussian-type-orbital basis sets,[40,48] in combination with the auxiliary Def2-TZVP/J basis sets[41] for the electron density fitting (RI) approximation.

Hyperfine coupling parameters were computed in the usual nonrelativistic first-order approach, using the MAG-ReSpect property package[49] employing unrestricted Kohn−Sham wave functions of the lowest triplet states of FMN in the above-described models, obtained with the TURBOMOLE program. The B3LYP hybrid functional[39,50,51] was employed in combination with the EPR-II basis set.[52]

RESULTS AND DISCUSSION

Solid-State Photo-CIDNP Mechanisms and Liquid-State NMR Spectra. Figure 1a shows a cyclic reaction scheme

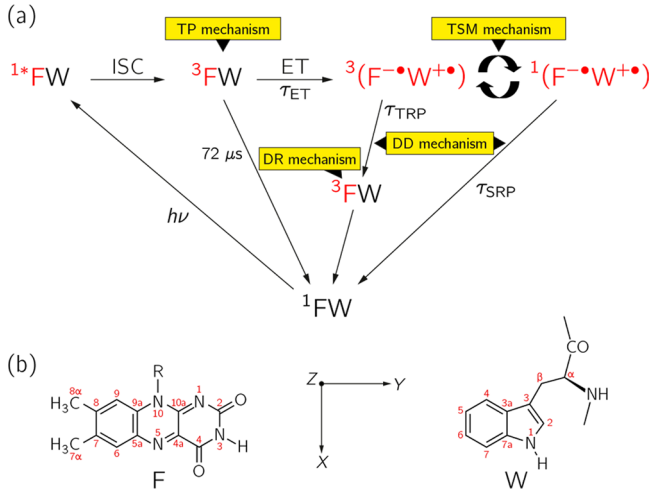

Figure 1. (a) Cyclic reaction scheme for the formation of photo-CIDNP in the LOV2-C450A mutant of phototropin, based on experimental observations by ^{13}C photo-CIDNP NMR[16,17] and time-resolved optical spectroscopy.[26] F: FMN cofactor. W: tryptophan-491 in the apoprotein.[17] ISC: intersystem crossing between excited singlet state of flavin, ^{1*}F, and triplet state of flavin, ^{3}F. TP mechanism: triplet polarization mechanism.[30] ET: electron transfer between W and ^{3}F, assumed to occur with a time constant τ_{ET} < 5 ns. Under this condition, $^3(F^{-\bullet}W^{+\bullet})$ acts as an independent photo-CIDNP source. TSM mechanism: three-spin mixing mechanism.[9,10] τ_{TRP}: lifetime of $^3(F^{-\bullet}W^{+\bullet})$. τ_{SRP}: lifetime of $^1(F^{-\bullet}W^{+\bullet})$. DD mechanism: differential decay mechanism.[12] DR mechanism: differential relaxation mechanism.[13] Note that ^{3}F generated by ISC and ^{3}F generated by charge recombination of $^3(F^{-\bullet}W^{+\bullet})$ may have different decay rates. (b) Molecular structures of F and W together with a coordinate system ***X***, ***Y***, ***Z***, that diagonalizes the electron dipolar tensor $\mathbf{D}^{TS}$ in ^{3}F. The numbers indicate the positions of the various ^{13}C hyperfine tensors $\mathbf{A}(i)$ in ^{3}F and $W^{+\bullet}$ (IUPAC numbering scheme).

for the LOV2-C450A mutant of phototropin that is consistent with experimental observations by ^{13}C photo-CIDNP NMR[16,17] and time-resolved optical absorption spectroscopy.[26] First, the ground state of the flavin cofactor is promoted into its excited singlet state by absorption of blue light. This is followed by intersystem crossing (ISC) to the triplet state, ^{3}F, which is generated with high quantum yield.[26] ^{3}F either decays to the ground state with an exponential time constant of 72 μs or

dx.doi.org/10.1021/jp507134y | J. Phys. Chem. B 2014, 118, 11622−11632

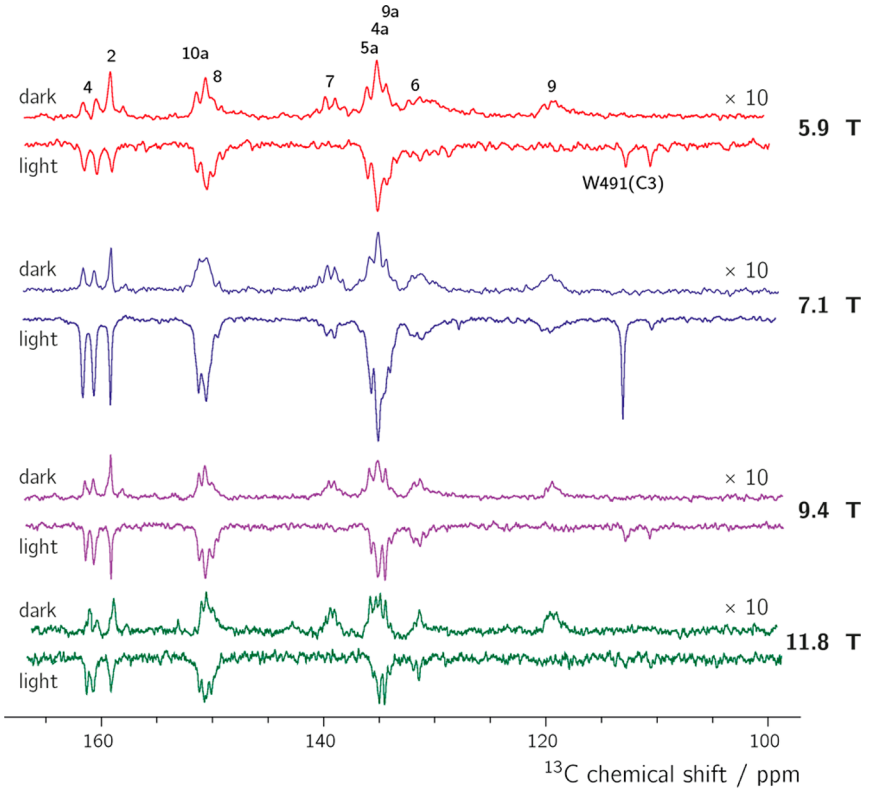

Figure 2. Solution ^{13}C NMR spectra of the LOV2-C450A mutant of phototropin, reconstituted with a universally ^{13}C-labeled FMN cofactor. The spectra refer to T = 278 K and four different magnetic fields ranging from B_0 = 5.9 to B_0 = 11.8 T. At each field, spectra were recorded both in the dark (upper spectra) and under blue light irradiation (lower spectra) using a nonselective $\pi/2$ pulse and composite pulse proton-decoupling. For convenience, the spectral intensities were corrected for the different number of scans used to record individual spectra. The numbers 2−10a indicate the assignment of the various ^{13}C signals to carbon atoms in the ^{13}C-labeled FMN cofactor (Figure 1b). A natural-abundance ^{13}C signal, observed only in the light spectra, is assigned to C(3) of W491 in the apoprotein (Figure 1b).[17]

abstracts an electron from tryptophan W491 to form a spin-correlated radical pair, $^3(F^{-\bullet}W^{+\bullet})$, in the triplet electron-spin configuration.[16,17] $^3(F^{-\bullet}W^{+\bullet})$ has two possible fates: It either evolves into an electronic singlet state, $^1(F^{-\bullet}W^{+\bullet})$, which subsequently undergoes (spin-allowed) charge recombination, or it undergoes backward electron transfer to ^3F and W. ^3F eventually decays to the ground state. Thus, there are two potential sources for photo-CIDNP in the studied LOV2 mutant: ^3F and $^3(F^{-\bullet}W^{+\bullet})$.

For a consistent analysis, one requires the relative contributions of triplet state (TS) flavin, ^3F, and triplet-configured radical pair (TRP), $^3(F^{-\bullet}W^{+\bullet})$, to photo-CIDNP formation. Here we describe these contributions by the branching ratio $R = x_{TS}/x_{TRP}$, where x_{TS} and x_{TRP} are the mole fractions of ^3F and $^3(F^{-\bullet}W^{+\bullet})$ in the sample. Values for R can be evaluated from the strength of a ^{13}C NMR reference signal in the 7.1-T photo-CIDNP spectra (see the Supporting Information, Table S1).

From Figure 1a, we infer that up to four different solid-state mechanisms can be effective in the LOV2-C450A mutant of phototropin. These mechanisms have one feature in common, in that they all require anisotropic hyperfine interactions

$$B = \Delta A \sin\theta_{hf}\cos\theta_{hf}$$
$$\Delta A = A_{ZZ} - \frac{1}{2}(A_{XX} + A_{YY}) \quad (1)$$

for the formation of photo-CIDNP. Here A_{XX}, A_{YY}, A_{ZZ}, and θ_{hf} are the principal values of the hyperfine tensor and the angle between the symmetry axis of the hyperfine tensor and the magnetic field, respectively [For simplicity, we assume an axially symmetric hyperfine tensor, i.e., $A_{XX} = A_{YY}$.]. For a protein in aqueous solution, all anisotropic magnetic interactions are modulated by unrestricted rotational diffusion of the macromolecule. Assuming a spherical protein shape, this motion can be characterized by a single rotational correlation time τ_C. If the correlation time of a protein satisfies the condition

$$\frac{1}{\Delta A} < \tau_C < \frac{1}{\Delta\sigma} \quad (2)$$

the chemical-shift anisotropy

$$\Delta\sigma = \sigma_{ZZ} - \frac{1}{2}(\sigma_{XX} + \sigma_{YY}) \quad (3)$$

is averaged to zero, whereas the far larger hyperfine anisotropy is conserved. Thus, under this condition, we expect to observe liquid-state ^{13}C NMR spectra with signal enhancements that arise from solid-state photo-CIDNP mechanisms. For a large photosynthetic protein with a molecular size of ∼1 MDa, this conjecture has recently been confirmed.[53] To check whether the condition (2) also applies to the LOV2 domains of phototropin (15−20 kDa), we acquired ^{13}C photo-CIDNP spectra of the LOV2-C450A mutant in the liquid state and in the solid phase with comparable parameters. Comparison reveals very similar polarization patterns in the two ^{13}C NMR spectra (see Supporting Information, Figure S1). This implies that photo-CIDNP observed in liquid-state NMR spectra of

dx.doi.org/10.1021/jp507134y | J. Phys. Chem. B 2014, 118, 11622−11632

LOV2 domains can reliably be analyzed using solid-state mechanisms.

Assignment of Observed ^{13}C NMR Signals. In Figure 2, we show solution ^{13}C NMR spectra of the LOV2-C450A mutant of phototropin, reconstituted with a universally ^{13}C-labeled FMN cofactor. The spectra refer to T = 278 K and four different magnetic fields, ranging from B_0 = 5.9 T to B_0 = 11.8 T. At each magnetic field, spectra were recorded both in the dark and under blue light irradiation (445 nm) using a nonselective $\pi/2$ pulse and composite pulse proton decoupling. For convenience, the spectral intensities in Figure 2 have been corrected for the different number of scans used to record the individual spectra.

In the NMR spectra measured in the dark, most of the ^{13}C atoms of the FMN chromophore appear as multiplets due to spin−spin coupling between the ^{13}C nuclei. On the basis of isotopolog editing using single-labeled and double-labeled FMN in conjunction with the coupling patterns in samples containing universally ^{13}C-labeled FMN, all ^{13}C NMR signals of the flavin cofactor could be unequivocally assigned (see IUPAC numbering scheme in the dark NMR spectrum recorded at 5.9 T).[16] Notably, the multiplet signals of the carbons 4a, 5a, and 9a overlap since their chemical shifts are closely similar. Likewise, the multiplets of 8 and 10a overlap.

Upon blue light irradiation, all [U-$^{13}C_{17}$]FMN NMR signals appear with negative signal amplitude. However, the intensity ratios between signals measured in the dark and under blue light condition vary over a wide range. Moreover, the signal enhancement of each FMN carbon atom also depends on the NMR magnetic field B_0.

Notably, a strong emissive NMR signal is observed in the light spectra around 111.8 ppm, which is absent in the dark, and which is not due to the resonance of any of the carbons within the [U-$^{13}C_{17}$]FMN chromophore. On the basis of natural-abundance ^{13}C photo-CIDNP studies on single and double mutant LOV2 domains, the signal has been assigned to C(3) of tryptophan W491 in the apoprotein (Figure 1b).[17] This carbon carries the highest electron spin density in the tryptophan radical W$^{+\bullet}$.[54] The signal of this ^{13}C nucleus becomes strongly polarized as a result of photoinitiated radical pair formation by electron transfer from W491 to ^{3}F. Due to spin conservation in a fast photochemical reaction, this radical pair is born in a triplet electron spin configuration.

Triplet Radical Pair Derived Photo-CIDNP. In this section, we discuss photo-CIDNP originating from a triplet radical pair, in which the singlet−triplet energy gap is relatively small and comparable with the hyperfine interactions. Generally, the experimental enhancement factor $\varepsilon^{exp}(i)$ of a given ^{13}C nucleus i is determined from the signal amplitude observed under light irradiation and in the dark

$$\varepsilon^{exp}(i) = (I_{light}(i) - I_{dark}(i))/I_{dark}(i) \quad (4)$$

In the LOV2-C450A mutant of phototropin, both ^{3}F and ^{3}(F$^{-\bullet}$W$^{+\bullet}$) may contribute to the light-induced nuclear spin polarization. If the electron-transfer step between W491 and ^{3}F is fast on the time scale of the nuclear quantum oscillations in ^{3}F,[30] i.e., τ_{ET} < 5 ns, the observed photo-CIDNP can be analyzed in terms of two separate sources. [If the electron transfer is fast on the time scale of the nuclear quantum oscillations in ^{3}F,[30] i.e., if τ_{ET} < 5 ns, "triplet nuclear spin polarization" can neither be formed nor be transferred to ^{3}(F$^{-\bullet}$W$^{+\bullet}$).[55] Thus, under this condition, ^{3}(F$^{-\bullet}$W$^{+\bullet}$) acts as a separate photo-CIDNP source. We believe that an electron-transfer time of τ_{ET} < 5 ns is compatible with the distance of 13.7 Å between W491 and FMN.[46]] Thus, under this condition, the experimental enhancement factor $\varepsilon^{exp}(i)$ is a weighted sum of the enhancement factors $\varepsilon^{exp}_{TS}(i)$ and $\varepsilon^{exp}_{TRP}(i)$ of the two photo-CIDNP sources

$$\varepsilon^{exp}(i) = \varepsilon^{exp}_{TS}(i)x_{TS} + \varepsilon^{exp}_{TRP}(i)x_{TRP} \quad (5)$$

Figure 1a implicates that photo-CIDNP in the W491 can arise only from a radical pair mechanism. In this case, eq 5 simplifies to

$$\varepsilon^{exp}_{TRP}(i) = \varepsilon^{exp}(i)/x_{TRP} \quad (6)$$

which enables the study of the "radical pair polarization" exclusive of the triplet source. Figure 3a shows the enhancement factor of ^{13}C−W(C3) at four different magnetic fields ranging from B_0 = 5.9 T to B_0 = 11.8 T: Starting out with an

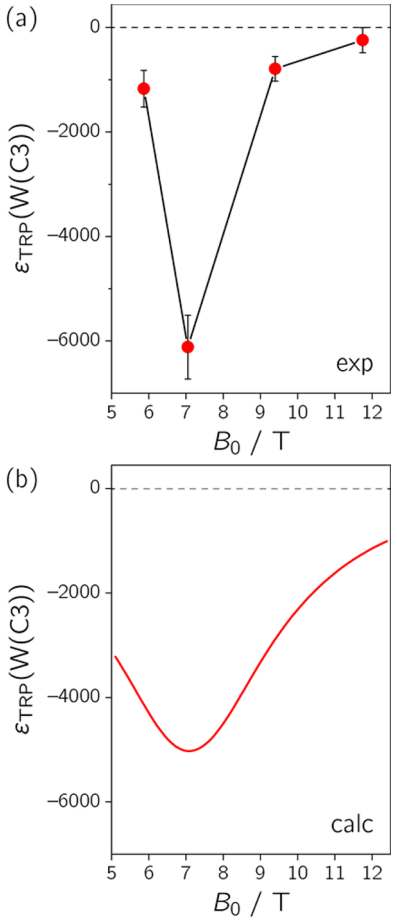

Figure 3. (a) Experimental enhancement factors ε^{exp}_{TRP}(W(C3)) of C(3) in W491 at four different magnetic fields ranging from B_0 = 5.9 T to B_0 = 11.8 T. Black solid lines are guides to the eyes. The error bars indicate the statistical errors of the photo-CIDNP experiments. Analysis shows that the observed photo-CIDNP can be attributed exclusively to ^{3}(F$^{-\bullet}$W$^{+\bullet}$). (b) Calculated enhancement factors ε^{cal}_{TRP}(W(C3)) as a function of the magnetic field in the range 5 T ≤ B_0 ≤ 12.5 T. The calculations were performed for ^{3}(F$^{-\bullet}$[3-^{13}C]W$^{+\bullet}$), using the three-spin mixing mechanism and an electron exchange parameter of J_{ex} = −38.4 MHz. The other geometric and magnetic parameters, underlying the calculations, were adopted from X-ray diffraction and EPR studies as well as from DFT computations (see the Supporting Information, Tables S2 and S3).

dx.doi.org/10.1021/jp507134y | J. Phys. Chem. B 2014, 118, 11622−11632

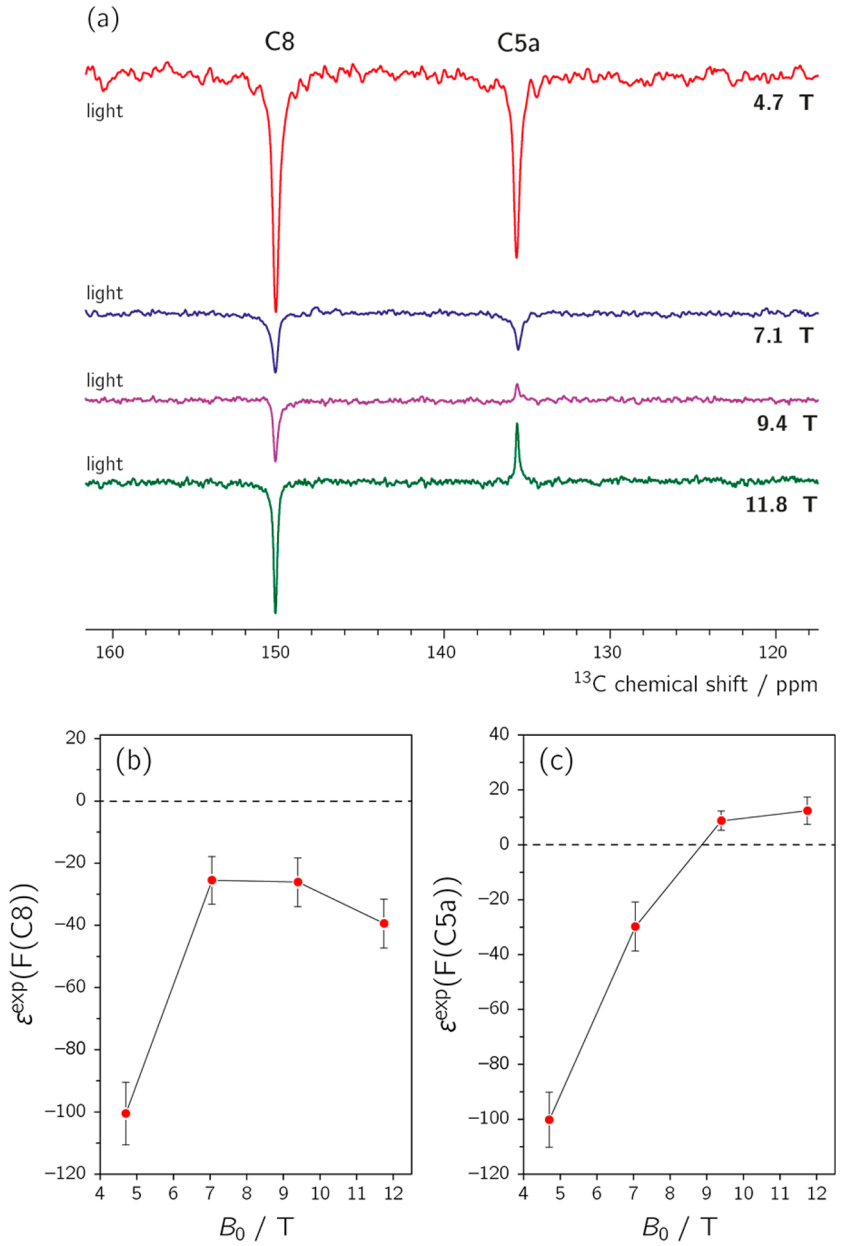

Figure 4. (a) Solution ^{13}C NMR spectra of the LOV2-C450A mutant of phototropin, reconstituted with a specifically ^{13}C-labeled cofactor carrying ^{13}C nuclei only in position F(C5a) and F(C8) (Figure 1b). The spectra refer to T = 278 K and four different magnetic fields ranging from B_0 = 4.7 T to B_0 = 11.8 T. At each field, spectra were recorded under blue light irradiation using a nonselective $\pi/2$ pulse and composite pulse proton decoupling. Generally, positive signals indicate absorptive and negative signals emissive nuclear spin polarization. Experimental enhancement factors $\varepsilon^{exp}(i)$ for ^{13}C−F(C8) (b) and ^{13}C−F(C5a) (c) in the FMN cofactor at four different magnetic fields ranging from B_0 = 4.7 T to B_0 = 11.8 T. Black solid lines are guides to the eyes. The error bars indicate the statistical errors of the photo-CIDNP experiments. Analysis reveals that at fields B_0 < 9 T, both $^3(F^{-\bullet}W^{+\bullet})$ and ^{3}F contribute to photo-CIDNP formation. However, due to the steep decrease of the "radical pair polarization" at magnetic fields above the emissive maximum (Figure 3), at B_0 = 11.8 T triplet flavin constitutes the dominant photo-CIDNP source.

enhancement factor of −1200, ε^{exp}_{TRP}(W(C3)) first gets more negative by a factor of 5, passes through a deep emissive maximum at 7.1 T and then steeply increases toward zero. [The enhancement factors ε^{exp}_{TRP}(W(C3)) were extracted from light and dark ^{13}C NMR spectra of the LOV2-C450A mutant of phototropin reconstituted with a universally ^{13}C-labeled FMN cofactor. For convenience, the NMR signal of ^{13}C−F(C2) was used as dark signal. Thus, due to the natural abundance of ^{13}C of 1.07%, all ε^{exp}_{TRP}(W(C3)) values, shown in Figure 3a, are scaled up by a factor of 100.] Similar magnetic-field dependencies have been observed for the ^{13}C nuclei in the primary radical pair of bacterial photosynthesis.[56]

Basically, photo-CIDNP in ^{13}C−W(C3) can be due to three different radical pair mechanisms: three-spin mixing,[9−11] differential decay,[12] and differential relaxation.[13,14] So far, however, the differential-relaxation mechanism could be established only in frozen solutions of photosynthetic reaction centers and at low magnetic fields, where nuclear-spin relaxation in the special pair (donor) triplet, ^{3}D, formed by charge recombination of the triplet-configured radical pair, $^3(D^{+\bullet}\ A^{-\bullet})$, is sufficiently fast.[14] Since our photo-CIDNP

dx.doi.org/10.1021/jp507134y | J. Phys. Chem. B 2014, 118, 11622−11632

experiments have been performed at liquid-state conditions and high magnetic fields, we neglect differential relaxation as a potential mechanism and restrict the discussion to three-spin mixing and differential decay.

In both remaining mechanisms, electron spin order is transferred to nuclear polarization by the anisotropic components of the hyperfine interaction. For the three-spin mixing mechanism, in addition an electron spin−spin coupling

$$d = -2J_{ex} + D^{RP}\left(\cos^2\theta_{ed} - \frac{1}{3}\right) \quad (7)$$

is required. Here, J_{ex}, D^{RP}, and θ_{ed} are the isotropic electron exchange interaction, the zero-field splitting parameter of the radical pair, and the angle between the symmetry axis of the electron dipolar tensor and the magnetic field, respectively. In the differential decay mechanism, anisotropic hyperfine interactions may cause a photo-CIDNP effect even in the absence of electron−electron coupling, if the radical pairs have different lifetimes in their triplet and singlet states

$$\tau_{TRP} \neq \tau_{SRP} \quad (8)$$

The two radical pair mechanisms can be distinguished on the basis of their different sign rules.[11] In the differential-decay mechanism, the relative photo-CIDNP enhancement of a given nucleus i depends on the sign of the secular hyperfine coupling $A(i)$, whereas in the three-spin mixing mechanism $\mathrm{sgn}(\varepsilon^{TSM}(i))$ is independent of $\mathrm{sgn}(A(i))$. From the uniform sign of all enhancement factors at $B_0 \leq 7.1$ T, we conclude that the three-spin mixing is the dominant radical pair mechanism in $^3(F^{+\bullet}W^{-\bullet})$.

In this mechanism, a global maximum of the photo-CIDNP effect is expected if the nuclear Larmor frequency ω_N matches the electron spin−spin coupling,[11]

$$|\omega_N| = |d| \quad (9)$$

Thus, if D^{RP} is known from an independent experiment, the electron exchange parameter J_{ex} can be extracted from the corresponding matching field

$$B_{match} = |d\hbar|/|g_N\beta_N| \quad (10)$$

Here g_N is the nuclear g-factor and β_N denotes the nuclear magneton. However, because of the two possible signs of J_{ex}, a 2-fold ambiguity exists. This ambiguity can be resolved using the sign rule of the three-spin-mixing mechanism[11]

$$\mathrm{sgn}(\varepsilon^{TSM}(i)) = -\mu\ \mathrm{sgn}(d)$$
$$\mu = +1\text{: initial triplet state}$$
$$\mu = -1\text{: initial singlet state} \quad (11)$$

Thus, a unique value for J_{ex} is obtained. Finally, an average lifetime τ_{RP} of the radical pair can be determined by a computer fit of the calculated enhancement factors of ^{13}C−W(C3) to the experiment. Since a full discussion of the photo-CIDNP formation in $^3(F^{-\bullet}W^{+\bullet})$ goes beyond the scope of this contribution, it is deferred to a separate publication. Here we present only the final result.

The fixed magnetic and geometric parameters of $^3(F^{-\bullet}$[3-^{13}C] $W^{+\bullet})$, underlying the analysis, were adopted from X-ray diffraction and EPR studies as well as from DFT computations (see the Supporting Information, Tables S2 and S3). Values for J_{ex} and τ_{RP} were obtained in the present study as outlined above. In Figure 3, we compare experimental enhancement factors of ^{13}C−W(C3) (a) with the best-fit simulation (b) based on the parameter values

$$J_{ex} = (-38.4 \pm 0.5)\mathrm{MHz},\ \tau_{RP} = (30 \pm 20)\mathrm{ns}$$

One sees that the calculated curve is in reasonable agreement with the observed magnetic-field dependence. This suggests that the photo-CIDNP analysis is basically correct. Nevertheless, some deviations still exist. In principle, these may be caused by minor contributions of the differential decay mechanism,[56] which requires a differential decay of the radical pairs in their triplet and singlet states.[12] So far, however, these lifetimes are not known for $^3(F^{-\bullet}W^{+\bullet})$ and $^1(F^{-\bullet}W^{+\bullet})$ in the LOV2 mutant of phototropin (see Figure 1a).

Triplet-State Derived Photo-CIDNP. In general, triplet states are characterized by a large singlet−triplet energy gap exceeding the magnetic interactions by orders of magnitude. As a consequence, the formation of photo-CIDNP in triplet states is different from that in triplet radical pairs. In the following, we explore photo-CIDNP effects induced in the ^{13}C atoms of the FMN cofactor. Particular emphasis is given to ^{3}F as potential new photo-CIDNP source. Because of their large hyperfine anisotropy, ^{13}C−F(C4a), ^{13}C−F(C5a), ^{13}C−F(C8), and ^{13}C−F(C9a) were chosen as probe nuclei for this study. To minimize cross-polarization,[57] which transfers light-induced magnetization to adjacent ^{13}C nuclei, the photo-CIDNP experiments were performed on protein samples with *specifically* ^{13}C-labeled FMN cofactors, such as [2,4a-$^{13}C_2$]FMN, [5a,8-$^{13}C_2$]FMN and [5a,7,8,9a-$^{13}C_4$]FMN. Generally, cross-polarization effects are negligible for ^{13}C nuclei that are not at close distance.

In Figure 4a we depict solution ^{13}C NMR spectra of the LOV2-C450A mutant carrying ^{13}C nuclei only in position 5a and 8 of the FMN cofactor. The spectra were recorded under blue light irradiation and refer to four different magnetic fields, ranging from B_0 = 4.7 T to B_0 = 11.8 T. Inspection of Figure 4 reveals that both the intensity and the sign of the NMR signals vary with the NMR measuring field.

In Figure 4b,c, we show the magnetic-field dependence of the enhancement factors of ^{13}C−F(C8) and ^{13}C−F(C5a). One sees that, in the field range from 4.7 to 7.1 T, the absolute value of ε^{exp}(F(C8)) first decreases by a factor of 4, passes through an emissive minimum at 7.1 T, and then increases again. Similarly, the enhancement factor of ^{13}C−F(C5a) first steeply decreases, then goes through zero, and at fields of B_0 > 9 T takes on positive values. Clearly, this magnetic-field dependence cannot be explained by a single photo-CIDNP source. Rather, the results indicate contributions from both possible sources, i.e., from $^3(F^{-\bullet}W^{+\bullet})$ and ^{3}F.

To specify the role of ^{3}F, photo-CIDNP calculations were performed on the basis of the triplet polarization (TP) mechanism.[30] In this mechanism, high nuclear spin polarization is generated solely by light excitation. The formation of this polarization is a consequence of the ISC and does not require intense microwave irradiation. Analysis reveals that the nuclear spins participate in the ISC process.[30] This gives rise to the formation of electron−nuclear spin ordering in zero-field which is transferred to oscillatory nuclear spin polarization by the anisotropic components of the hyperfine interaction in the presence of a magnetic field.

To analyze the photo-CIDNP data, we calculate the stationary nuclear spin polarization after a single excitation cycle

dx.doi.org/10.1021/jp507134y | J. Phys. Chem. B 2014, 118, 11622−11632

$$I_z^{stat}(\Omega) = (1/\tau_T)\int_0^{5\tau_T} \exp(-t/\tau_T) I_z(\Omega, t)\, dt \quad (12)$$

which is a good approximation to the steady-state polarization that builds up on condition of continuous optical pumping. Here, τ_T is the lifetime of ^{3}F, $I_z(\Omega,t)$ indicates the oscillatory nuclear spin polarization induced by light excitation,[30] and Ω denotes the orientation of ^{3}F in the laboratory frame, x, y, z, with B_0 along the z-axis. In our model, the orientation dependence of the magnetic tensor elements in the laboratory frame is evaluated by a 2-fold transformation. In the first step, we transform from the principal axis system X_i, Y_i, Z_i, of the respective magnetic tensor to a magnetic reference system X, Y, Z, using the Euler angles $\Omega_i = (\Phi_i,\Theta_i,\Psi_i)$. For convenience, this reference system is chosen parallel to the principal axis system of the electron dipolar tensor of ^{3}F. In the second step, we transform by the Euler angles $\Omega = (\Phi,\Theta,0)$ into the laboratory frame x, y, z. A random distribution of ^{3}F with respect to the laboratory frame is considered by averaging over Φ and Θ

$$I_z^{stat} = \int_{\Theta=0}^{\pi}\int_{\Phi=0}^{2\pi} I_z^{stat}(\Phi,\Theta)\, d\Phi \sin\Theta\, d\Theta \quad (13)$$

The magnetic and kinetic parameters underlying the calculations are available from independent experiments and DFT computations. Figure 1b depicts the molecular structure of FMN together with a coordinate system X, Y, Z, that diagonalizes the electron dipolar tensor $\mathbf{D}^{TS}$ in ^{3}F. [So far, the orientation of the electron dipolar tensor of ^{3}F in the LOV2-C450A mutant of phototropin has not been determined. We therefore assume that this tensor has the same orientation as the g-tensor in the neutral flavin radical, FH$^\bullet$.[58] For simplicity, however, the X- and Y-axes of the electron dipolar tensor are rotated by −14° about Z relative to the orientation of the g-tensor of FH$^\bullet$.] The eigenvalues of $\mathbf{D}^{TS}$ can be written as $D_{XX}^{TS} = -(1/3)D^{TS} + E^{TS}$, $D_{YY}^{TS} = -(1/3)D^{TS} - E^{TS}$ and $D_{ZZ}^{TS} = (2/3)D^{TS}$. In Table 1, we list the zero-field parameters D^{TS}, E^{TS},

Table 1. Zero-Field Splitting Parameters and Zero-Field Populations of Neutral ^{3}FMN in the LOV2-C450A-Mutant of Phototropin Evaluated by Transient EPR at Cryogenic Temperatures[a]

zero-field splitting parameters/MHz[b]		zero-field populations	
$\lvert D^{TS}\rvert$	1695.8	p_X	0.63
$\lvert E^{TS}\rvert$	524.3	p_Y	0.37
		p_Z	0.0

[a]Adopted from ref 59. [b]The signs of D^{TS} and E^{TS} are not determined by the transient EPR experiments.

and zero-field populations p_X, p_X, and p_Z of neutral ^{3}F in the LOV2 mutant of phototropin. The parameters were evaluated using transient EPR at cryogenic temperatures.[59] Table 2 summarizes the corresponding parameters of protonated ^{3}F adapted from a transient EPR study of photoexcited ^{3}F in frozen aqueous solution.[60] The signs of D^{TS} and E^{TS} were not determined by the time-resolved EPR experiments but were arbitrarily fixed to $D^{TS} > 0$ and $E^{TS} < 0$ in the photo-CIDNP calculations. With the other possible assignment of $D^{TS} > 0$ and $E^{TS} > 0$, we obtained very similar nuclear spin polarizations differing only by ±10%.

The numbers 4a, 5a, 8, and 9a in the molecular structure of FMN denote the positions of the four ^{13}C probe nuclei of this study (see Figure 1b). For simplicity, we assume that the

Table 2. Zero-Field Splitting Parameters and Zero-Field Populations of Protonated ^{3}FMN in Frozen Aqueous Solution Evaluated by Transient EPR at Cryogenic Temperatures[a]

zero-field splitting parameters/MHz[b]		zero-field populations	
$\lvert D^{TS}\rvert$	1884.7	p_X	0.50
$\lvert E^{TS}\rvert$	515.4	p_Y	0.0
		p_Z	0.50

[a]Adopted from ref 60. [b]The signs of D^{TS} and E^{TS} are not determined by the transient EPR experiments.

principal axes of the corresponding hyperfine tensors $\mathbf{A}(i)$ coincide with the zero-field splitting tensor axes. The hyperfine components $A_{XX}(i)$, $A_{YY}(i)$, and $A_{ZZ}(i)$ were obtained by DFT computations, using the BP86 functional for geometry optimization and the B3LYP functional for hyperfine calculations.[35−44,50−52] Table 3 summarizes the ^{13}C hyperfine

Table 3. Computed ^{13}C Principal Values of the Hyperfine Tensor of ^{3}FMN in MHz

	isolated ^{3}FMN[a]			^{3}FMN in protein environment[b]		
^{13}C nuclear position i	$A_{XX}(i)$	$A_{YY}(i)$	$A_{ZZ}(i)$	$A_{XX}(i)$	$A_{YY}(i)$	$A_{ZZ}(i)$
C4a	−6.17	−4.76	+35.31	−8.97	−7.27	+16.25
C5a	−11.21	−8.97	−1.68	−9.81	−7.85	+1.40
C8	+0.56	+1.12	+32.79	−1.68	−1.12	+19.61
C9a	−4.20	−3.92	+15.41	−5.88	−5.61	+17.38

[a]Calculations performed in this study using the BP86 functional for geometry optimization and the B3LYP functional for hyperfine calculations. [b]Calculations performed in this study assuming vertical excitation from the singlet structure.

tensor elements of neutral ^{3}FMN calculated for an isolated triplet state and lists the ^{13}C hyperfine parameters of ^{3}FMN in the hydrogen-bond network of the protein environment. The parameters were obtained by considering interactions with five neighboring amino acids (see Materials and Methods, DFT Computations). Values for the lifetime τ_T of ^{3}FMN in the LOV2 domains of phototropin were adopted from a transient absorption study.[26]

Figure 5 shows the stationary nuclear spin polarization of ^{13}C−F(C4a), ^{13}C−F(C5a), ^{13}C−F(C8), and ^{13}C−F(C9a), calculated for the TP mechanism as a function of the polarization field in the range of B_0 = 0 to 12 T. The calculations refer to isolated ^{3}FMN in a powder sample characterized by a random distribution of the triplet state in the laboratory frame. One sees that the nuclear spin polarization of each ^{13}C nucleus exhibits a distinct emissive maximum at lower magnetic fields. This behavior corresponds to the predictions of the analytical model based on the high-field approximation.[30] In this model, a maximum of I_z^{stat} is expected if the nuclear Larmor frequency ω_N matches the secular hyperfine coupling $A(i)$ of a given ^{13}C nucleus[30]

$$|\omega_N| = |A(i)|$$

$$A(i) = A_{iso}(i) + \Delta A(i)\left(\cos^2\theta_{hf} - \frac{1}{3}\right). \quad (14)$$

Here, $A_{iso}(i)$, $\Delta A(i)$, and θ_{hf} are the isotropic hyperfine coupling constant, the hyperfine anisotropy and the angle

dx.doi.org/10.1021/jp507134y | J. Phys. Chem. B 2014, 118, 11622−11632

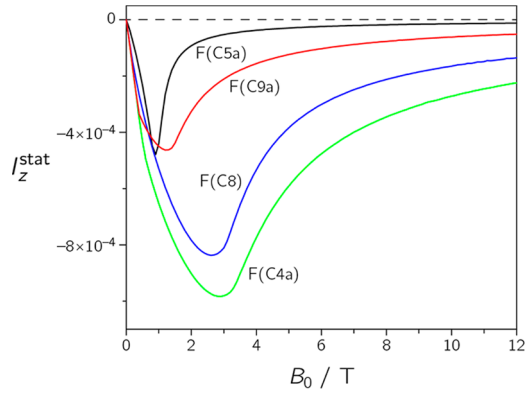

Figure 5. Stationary nuclear spin polarization I_z^{stat} of the triplet state, calculated for ^{13}C−F(C4a), ^{13}C−F(C5a), ^{13}C−F(C8), and ^{13}C−F(C9a) as a function of the polarization field from $B_0 = 0$ to $B_0 = 12$ T. The calculations refer to neutral ^{3}FMN (Tables 1 and 3) in powder samples characterized by a random distribution of the triplet states in the laboratory frame. Maximum polarization is expected if the nuclear Larmor frequency matches the secular hyperfine coupling of a particular ^{13}C nucleus, $|\omega_N| = |A(i)|$.[30]

between the symmetry axis of the hyperfine tensor and the magnetic field, respectively. ^{13}C−F(C5a) has the smallest hyperfine parameters and thus shows the lowest matching field

$$B_{match}(i) = |A(i)\hbar|/|g_N\beta_N| \quad (15)$$

In contrast, ^{13}C−F(C4a) has the largest hyperfine parameters and consequently exhibits the highest matching field. For $B_0 \gg B_{match}$, the analytical model predicts a linear dependence of I_z^{stat} on the inverse strength of the magnetic field, $I_z^{stat} \approx B_0^{-1}$.[30] This weak field dependence guarantees large stationary enhancement factors

$$\varepsilon^{cal}(i) = I_z^{stat}(i)/I_z^{eq} \quad (16)$$

even at very high magnetic fields. Thus, due to the steep decrease of the "radical pair polarization" after the emissive maximum (see Figure 3), we expect that at $B_0 = 11.8$ T triplet flavin constitutes the dominant photo-CIDNP source, i.e.

$$|\varepsilon_{TRP}^{exp}(i)x_{TRP}| \ll |\varepsilon_{TS}^{exp}(i)x_{TS}| \quad (17)$$

and

$$\varepsilon_{TS}^{exp}(i) \approx \varepsilon^{exp}(i)/x_{TS} \quad (18)$$

Figure 6a shows the experimental enhancement factors $\varepsilon_{TS}^{exp}(i)$ of the triplet state for ^{13}C−F(C4a), ^{13}C−F(C5a), ^{13}C−F(C8), and ^{13}C−F(C9a) evaluated at a polarization field of $B_0 = 11.8$ T. To minimize cross-polarization effects,[57] all photo-CIDNP experiments were performed on LOV2 mutants reconstituted with specifically ^{13}C-labeled FMN cofactors. One sees large enhancement factors varying between $\varepsilon_{TS}^{exp} = +20$ for ^{13}C−F(C5a) and $\varepsilon_{TS}^{exp} = -65$ for ^{13}C−F(C8). In Figure 6b, we depict the calculated enhancement factors for the same four ^{13}C nuclei. The calculations refer to the zero-field parameters, zero-field populations, and hyperfine parameters of neutral ^{3}FMN in the LOV2 mutant of phototropin (Tables 1 and 3). In general, the calculated enhancement factors agree reasonably with their experimental counterparts.

It should be noted, however, that ^{13}C−F(C5a) exhibits a positive enhancement factor whereas the calculation (Figure 6b) indicates a negative sign. The discrepancy might be connected with the protonation state of ^{3}FMN, which is not

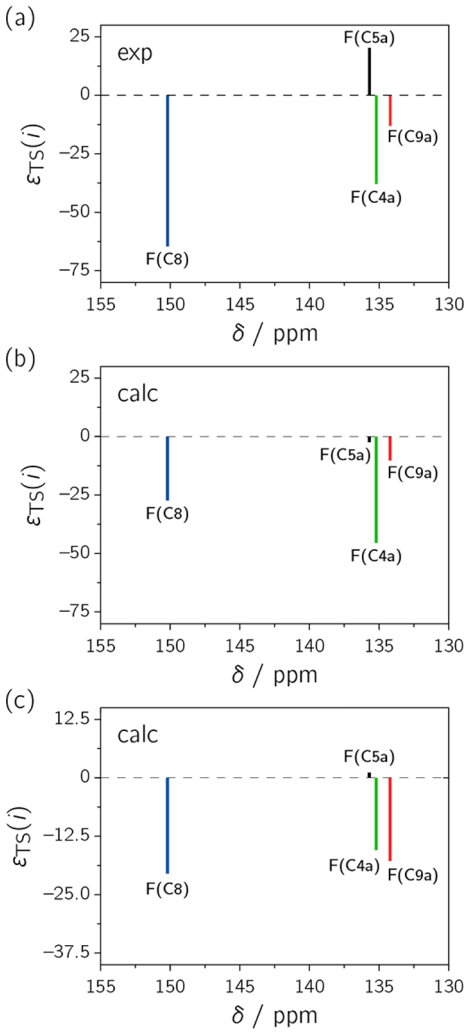

Figure 6. (a) Experimental enhancement factors $\varepsilon_{TS}^{exp}(i)$ of the triplet state, evaluated for ^{13}C−F(C4a), ^{13}C−F(C5a), ^{13}C−F(C8), and ^{13}C−F(C9a) at a polarization field of $B_0 = 11.8$ T. (b) Calculated enhancement factors $\varepsilon_{TS}^{cal}(i)$ of the triplet state for the same four ^{13}C probe nuclei at $B_0 = 11.8$ T. The calculations refer to neutral ^{3}FMN (Tables 1 and 3) in powder samples. (c) Calculated enhancement factors $\varepsilon_{TS}^{cal}(i)$ of the triplet state for the same four ^{13}C probe nuclei at $B_0 = 11.8$ T. The calculations refer to protonated ^{3}FMN (Tables 2 and 3) in powder samples. The chemical shifts of the respective NMR resonances have been taken from refs 16 and 27.

known for the LOV2 mutant under the experimental conditions ($T = 278$ K, pH = 7.0). For conventional triplet states with $|D^{TS}| \gg |E^{TS}|$, the sign rule of the TP mechanism is given by

$$\mathrm{sgn}(\varepsilon_{TS}(i)) = \mathrm{sgn}(p_Y - p_X)\mathrm{sgn}(E^{TS})\mathrm{sgn}(A_{ZZ}(i)) \quad (19)$$

On condition that $|D^{TS}| \approx 3|E^{TS}|$, which applies to ^{3}FMN, $\mathrm{sgn}(\varepsilon_{TS}(i))$ depends on the sign and magnitude of all three population differences $(p_Y - p_Z)$, $(p_X - p_Z)$, and $(p_Y - p_X)$ as well as on the sign and magnitude of all hyperfine components. In this case, a simple sign rule does not exist anymore and $\mathrm{sgn}(\varepsilon_{TS}(i))$ can be evaluated only numerically. Using the zero-field populations of neutral ^{3}FMN, $p_X = 0.63$, $p_Y = 0.37$, and $p_Z = 0$,[59] yields negative enhancement factors for all four ^{13}C probe nuclei (see Figure 5). We then assume that ^{3}FMN is protonated under the experimental conditions, $p_X = 0.50$, $p_Y =$

dx.doi.org/10.1021/jp507134y | J. Phys. Chem. B 2014, 118, 11622−11632

0, and p_Z = 0.50,[60] and obtain a negative sign for ε_{TS}(C(4a)), ε_{TS}(C(8)), and ε_{TS}(C(9a)) but a positive sign for ε_{TS}(C(5a)).

To assess this result, we performed DFT computations for ^{1}FMN considering the protein surroundings. In particular, interactions with the five neighboring amino acids Q454, N482, N492, Q513, and N449 were taken into account (see Materials and Methods, DFT Computations). Analysis revealed formation of five hydrogen bonds between these amino acids and the isoalloxazine ring of ^{1}FMN with H···O bond lengths ranging from 1.83 to 2.35 Å. Interestingly, four of these hydrogen bonds are proton donors, which transfer positive charge density to ^{1}FMN. Thus, in case of vertical excitation from the singlet structure, partially protonated ^{3}FMN is generated upon light irradiation. In Figure 6c, we depict the enhancement factors for ^{13}C−F(C4a), ^{13}C−F(C5a), ^{13}C−F(C8), and ^{13}C−F(C9a) calculated with the zero-field populations and hyperfine parameters of ^{3}FMN in the protein environment (Tables 2 and 3). One sees that ^{13}C−F(C5a) is now absorptively polarized whereas the other three ^{13}C nuclei are emissively polarized, as observed in the photo-CIDNP experiments (Figure 6a). This suggests that ^{3}FMN in the LOV mutant is protonated under physiological conditions.

In Table 4, we compare the experimental enhancement factors of the triplet state with those calculated for protonated ^{3}FMN. It is important to emphasize that the "triplet polarization" cannot be studied exclusively. Rather, one observes always contributions from both possible sources. This leads to rather large systematic errors of ±50% for the experimental enhancement factors of the triplet state. In case of small ε_{TS}^{exp} values, these errors may even exceed ±100%. Similar large errors are expected also for the calculated enhancement factors, since the hyperfine parameters of ^{3}FMN, computed by DFT, may well deviate by 40−50% from the true values, which are, to the best of our knowledge, undetermined so far. Moreover, the zero-field populations of protonated ^{3}FMN, used in the calculations, have been determined in frozen aqueous solution[60] and may therefore differ from those in the LOV2 mutant at room temperature. In view of these uncertainties, the agreement between experimental (Table 4, column 2) and calculated enhancement factors (Table 4, column 4) is remarkably good. Thus, we have for the first time detected that a triplet state is the major source for photo-CIDNP in a photoactive protein.

Table 4. Comparison of Experimental and Calculated Enhancement Factors of ^{3}FMN in the LOV2-C450A-Mutant of Phototropin under Physiological Conditions

	experimental enhancement factor[a]		calculated enhancement factor[b]	
^{13}C nuclear position	ε_{TS}^{exp}	system. error	ε_{TS}^{cal}	system. error
C4a	−38	±19	−16	±8
C5a	+20	±16	+1	±0.5
C8	−65	±33	−21	±10
C9a	−8	±8	−18	±9

[a]Evaluated in this study at T = 278 K and B_0 = 11.8 T. [b]Calculated in this study for protonated ^{3}FMN using experimental zero-field parameters and zero-field populations (ref 60). The hyperfine parameters are adapted from DFT computations performed for a triplet state FMN in the protein environment.

CONCLUSIONS

The triplet state of the FMN cofactor, ^{3}FMN, has been identified as a new source for photo-CIDNP in the blue light receptor phototropin. From a quantitative analysis of the nuclear spin polarization detected in the diamagnetic cofactor, detailed information was obtained on the electronic structure of the triplet intermediate and its surroundings at atomic resolution. We expect that the photo-CIDNP technique presented in this study may help to clarify the mechanism of adduct formation in the wild-type LOV domains of phototropin. It is commonly accepted that ^{3}FMN is the key intermediate of this significant photoreaction.[26] So far, however, all other mechanistic and conformational steps are still a matter of considerable debate.[26,28,59,61−66]

Generally, photochemistry in photoactive proteins proceeds via spin-correlated radical pairs formed either in a singlet or in a triplet state. If, initially, a singlet radical pair is formed, the observed photo-CIDNP can by analyzed using a radical pair mechanism.[9−14] In the case of a triplet radical pair, however, nuclear spin polarization may be generated already in the precursor state.[30] Therefore, the spin dynamics in this intermediate should also be considered. This requires a more comprehensive analysis involving both a radical pair and the new triplet polarization mechanism. We believe that this approach is necessary for various photoactive proteins in which triplet states are generated upon photoexcitation,[26,59,67−69] to unravel the electron transfer pathways and to identify the redox partners involved in protein function, especially at higher magnetic fields.

ASSOCIATED CONTENT

Supporting Information

Details of the evaluation of the branching ratio; comparison of solution and solid-state ^{13}C photo-CIDNP NMR spectra; magnetic, geometric, and kinetic parameters used for the photo-CIDNP analysis of the triplet radical pair. This material is available free of charge via the Internet at http://pubs.acs.org.

AUTHOR INFORMATION

Corresponding Authors

*Phone: +49 761 203-6193. Fax: +49 761 203-6222; E-mail: Gerd.Kothe@physchem.uni-freiburg.de.

*Phone: +49 761 203-6213. Fax: +49 761 203-6222. E-mail: Stefan.Weber@physchem.uni-freiburg.de.

Notes

The authors declare no competing financial interest.

ACKNOWLEDGMENTS

We thank PD Dr. Erik Schleicher for valuable discussions and Constantin Schalck for the construction of the fiber-optic laser photoexcitaton device. This work was supported by grants of the Deutsche Forschungsgemeinschaft (DFG), WE 2376/4-1 and FI 824/6-1.

REFERENCES

(1) Kaptein, R.; Dijkstra, K.; Nicolay, K. Laser photo-CIDNP as a surface probe for proteins in solution. *Nature* **1978**, *274*, 293−294.

(2) Hore, P. J.; Broadhurst, R. W. Photo-CIDNP of biopolymers. *Prog. Nucl. Magn. Reson. Spectrosc.* **1993**, *25*, 345−402.

(3) Mok, K. H.; Hore, P. J. Photo-CIDNP NMR methods for studying protein folding. *Methods* **2004**, *34*, 75−87.

(4) Zysmilich, M. G.; McDermott, A. Photochemically induced dynamic nuclear polarization in the solid-state ^{15}N spectra of reaction

centers from photosynthetic bacteria *Rhodobacter sphaeroides* R-26. *J. Am. Chem. Soc.* **1994**, *116*, 8362−8363.
(5) Zysmilich, M. G.; McDermott, A. Natural abundance solid-state carbon NMR studies of photosynthetic reaction centers with photoinduced polarization. *Proc. Natl. Acad. Sci. U.S.A.* **1996**, *93*, 6857−6860.
(6) Alia; Roy, E.; Gast, P.; van Gorkom, H. J.; de Groot, H. J. M.; Jeschke, G.; Matysik, J. Photochemically induced dynamic nuclear polarization in photosystem I of plants observed by ^{13}C magic-angle spinning NMR. *J. Am. Chem. Soc.* **2004**, *126*, 12819−12826.
(7) Prakash, S.; Alia; Gast, P.; de Groot, H. J. M.; Matysik, J.; Jeschke, G. Photo-CIDNP MAS NMR in intact cells of *Rhodobacter sphaeroides* R26: molecular and atomic resolution at nanomolar concentration. *J. Am. Chem. Soc.* **2006**, *128*, 12794−12799.
(8) Roy, E.; Rohmer, T.; Gast, P.; Jeschke, G.; Alia, A.; Matysik, J. Characterization of the primary radical pair in reaction centers of *Heliobacillus mobilis* by ^{13}C Photo-CIDNP MAS NMR. *Biochemistry* **2008**, *47*, 4629−4635.
(9) Kothe, G.; Bechtold, M.; Link, G.; Ohmes, E.; Weidner, J.-U. Pulsed EPR detection of light-generated nuclear coherences in photosynthetic reaction centers. *Chem. Phys. Lett.* **1998**, *283*, 51−60.
(10) Jeschke, G. A new mechanism for chemically induced dynamic nuclear polarization in the solid state. *J. Am. Chem. Soc.* **1998**, *120*, 4425−4429.
(11) Jeschke, G.; Matysik, J. A reassessment of the origin of photochemically induced dynamic nuclear polarization effects in solids. *Chem. Phys.* **2003**, *294*, 239−255.
(12) Polenova, T.; McDermott, A. E. A coherent mixing mechanism explains the photoinduced nuclear polarization in photosynthetic reaction centers. *J. Phys. Chem. B* **1999**, *103*, 535−548.
(13) McDermott, A.; Zysmilich, M. G.; Polenova, T. Solid state NMR studies of photoinduced polarization in photosynthetic reaction centers: mechanism and simulations. *Solid State Nucl. Mag.* **1998**, *11*, 21−47.
(14) Thamarath, S. S.; Bode, B. E.; Prakash, S.; Gupta, K. B. S. S.; Alia, A.; Jeschke, G.; Matysik, J. Electron spin density distribution in the special pair triplet of *Rhodobacter sphaeroides* R26 revealed by magnetic field dependence of the solid-state photo-CIDNP effect. *J. Am. Chem. Soc.* **2012**, *134*, 5921−5930.
(15) Daviso, E.; Prakash, S.; Alia, A.; Gast, P.; Neugebauer, J.; Jeschke, G.; Matysik, J. The electronic structure of the primary electron donor of reaction centers of purple bacteria at atomic resolution as observed by photo-CIDNP ^{13}C NMR. *Proc. Natl. Acad. Sci. U.S.A.* **2009**, *106*, 22281−22286.
(16) Richter, G.; Weber, S.; Römisch, W.; Bacher, A.; Fischer, M.; Eisenreich, W. Photochemically induced dynamic nuclear polarization in a C450A mutant of the LOV2 domain of the *Avena sativa* blue-light receptor phototropin. *J. Am. Chem. Soc.* **2005**, *127*, 17245−17252.
(17) Eisenreich, W.; Joshi, M.; Weber, S.; Bacher, A.; Fischer, M. Natural abundance solution ^{13}C NMR studies of a phototropin with photoinduced polarization. *J. Am. Chem. Soc.* **2008**, *130*, 13544−13545.
(18) Eisenreich, W.; Fischer, M.; Römisch-Margl, W.; Joshi, M.; Richter, G.; Bacher, A.; Weber, S. Tryptophan ^{13}C nuclear-spin polarization generated by intraprotein electron transfer in a LOV2 domain of the blue-light receptor phototropin. *Biochem. Soc. Trans.* **2009**, *37*, 382−386.
(19) Thamarath, S. S.; Heberle, J.; Hore, P. J.; Kottke, T.; Matysik, J. Solid-state photo-CIDNP effect observed in phototropin LOV1-C57S by ^{13}C magic-angle spinning NMR spectroscopy. *J. Am. Chem. Soc.* **2010**, *132*, 15542−15543.
(20) Wang, X.; Thamarath, S. S.; Matysik, J. Magnetic field dependence of the solid-state photo-CIDNP effect observed in phototropin LOV1-C57S. *Acta Chim. Sin.* **2013**, *71*, 169−172.
(21) Demarsy, E.; Fankhauser, C. Higher plants use LOV to perceive blue light. *Curr. Opin. Plant Biol.* **2009**, *12*, 69−74.
(22) Christie, J. M.; Gawthorne, J.; Young, G.; Fraser, N. J.; Roe, A. J. LOV to BLUF: flavoprotein contributions to the optogenetic toolkit. *Mol. Plant* **2012**, *5*, 533−544.
(23) Hohm, T.; Preuten, T.; Fankhauser, C. Phototropism: translating light into directional growth. *Am. J. Bot.* **2013**, *100*, 47−59.
(24) Liscum, E.; Askinosie, S. K.; Leuchtman, D. L.; Morrow, J.; Willenburg, K. T.; Coats, D. R. Phototropism: growing towards and understanding of plant movement. *Plant Cell* **2014**, *26*, 38−55.
(25) Salomon, M.; Christie, J. M.; Knieb, E.; Lempert, U.; Briggs, W. R. Photochemical and mutational analysis of the FMN-binding domain of the plant blue light receptor, phototropin. *Biochemistry* **2000**, *39*, 9401−9410.
(26) Swartz, T. E.; Corchnoy, S. B.; Christie, J. M.; Lewis, J. W.; Szundi, I.; Briggs, W. R.; Bogomolni, R. A. The photocycle of a flavin-binding domain of the blue light photoreceptor phototropin. *J. Biol. Chem.* **2001**, *276*, 36493−36500.
(27) Salomon, M.; Eisenreich, W.; Dürr, H.; Schleicher, E.; Knieb, E.; Massey, V.; Rüdiger, W.; Müller, F.; Bacher, A.; Richter, G. An optomechanical transducer in the blue light receptor phototropin from *Avena sativa*. *Proc. Natl. Acad. Sci. U.S.A.* **2001**, *98*, 12357−12361.
(28) Kay, C. W. M.; Schleicher, E.; Kuppig, A.; Hofner, H.; Rüdiger, W.; Schleicher, M.; Fischer, M.; Bacher, A.; Weber, S.; Richter, G. Blue light perception in plants. Detection and characterization of a light-induced neutral flavin radical in a C450A mutant of phototropin. *J. Biol. Chem.* **2003**, *278*, 10973−10982.
(29) Kottke, T.; Dick, B.; Fedorov, R.; Schlichting, I.; Deutzmann, R.; Hegemann, P. Irreversible photoreduction of flavin in a mutated Phot-LOV1 domain. *Biochemistry* **2003**, *42*, 9854−9862.
(30) Kothe, G.; Yago, T.; Weidner, J.-U.; Link, G.; Lukaschek, M.; Lin, T.-S. Quantum oscillations and polarization of nuclear spins in photoexcited triplet states. *J. Phys. Chem. B* **2010**, *114*, 14755−14762.
(31) Römisch, W.; Eisenreich, W.; Richter, G.; Bacher, A. Rapid one-pot synthesis of riboflavin isotopomers. *J. Org. Chem.* **2002**, *67*, 8890−8894.
(32) Sedlmaier, H.; Müller, F.; Keller, P. J.; Bacher, A. Enzymatic-synthesis of riboflavin and FMN specifically labeled with ^{13}C in the xylene ring. *Z. Naturforsch. C* **1987**, *42*, 425−429.
(33) van Schagen, C. G.; Müller, F. A ^{13}C nuclear-magnetic-resonance study on free flavins and *Megasphaera elsdenii* and *Azotobacter vinelandii* flavodoxin. ^{13}C-enrichted flavins as probes for the study of flavoprotein active sites. *Eur. J. Biochem.* **1981**, *120*, 33−39.
(34) Dwyer, T. M.; Mortl, S.; Kemter, K.; Bacher, A.; Fauq, A.; Frerman, F. E. The intraflavin hydrogen bond in human electron transfer flavoprotein modulates redox potentials and may participate in electron transfer. *Biochemistry* **1999**, *38*, 9735−9745.
(35) Furche, F.; Ahlrichs, R. Adiabatic time-dependent density functional methods for excited state properties. *J. Chem. Phys.* **2002**, *117*, 7433−7447.
(36) Rappoport, D.; Furche, F. Analytical time-dependent density functional derivative methods within the RI-*J* approximation, an approach to excited states of large molecules. *J. Chem. Phys.* **2005**, *122*, 064105.
(37) Furche, F.; Rappoport, D. In *Computational Photochemistry*; Olivucci, M., Ed.; Elsevier: Amsterdam, 2005; pp 93−128.
(38) Perdew, J. P. Density-functional approximation for the correlation energy of the inhomogeneous electron gas. *Phys. Rev. B* **1986**, *33*, 8822−8824.
(39) Becke, A. D. Density-functional exchange-energy approximation with correct asymptotic behavior. *Phys. Rev. A* **1988**, *38*, 3098−3100.
(40) Weigend, F.; Häser, M.; Patzelt, H.; Ahlrichs, R. RI-MP2: optimized auxiliary basis sets and demonstration of efficiency. *Chem. Phys. Lett.* **1998**, *294*, 143−152.
(41) Weigend, F. Accurate Coulomb-fitting basis sets for H to Rn. *Phys. Chem. Chem. Phys.* **2006**, *8*, 1057−1065.
(42) Eichkorn, K.; Treutler, O.; Öhm, H.; Häser, M.; Ahlrichs, R. Erratum: Auxiliary basis-sets to approximate Coulomb potentials (Vol. 240, Pg. 283, 1995). *Chem. Phys. Lett.* **1995**, *242*, 652−660.
(43) Eichkorn, K.; Weigend, F.; Treutler, O.; Ahlrichs, R. Auxiliary basis sets for main row atoms and transition metals and their use to approximate Coulomb potentials. *Theor. Chem. Acc.* **1997**, *97*, 119−124.

(44) Sierka, M.; Hogekamp, A.; Ahlrichs, R. Fast evaluation of the Coulomb potential for electron densities using multipole accelerated resolution of identity approximation. *J. Chem. Phys.* **2003**, *118*, 9136−9148.
(45) TURBOMOLE V6.4 2012, a development of University of Karlsruhe and Forschungszentrum Karlsruhe GmbH, 1989−2007, TURBOMOLE GmbH, since 2007; available from http://www.turbomole.com.
(46) Halavaty, A. S.; Moffat, K. N- and C-terminal flanking regions modulate light-induced signal transduction in the LOV2 domain of the blue light sensor phototropin 1 from *Avena sativa*. *Biochemistry* **2007**, *46*, 14001−14009.
(47) Neese, F. ORCA. An ab initio, DFT and semiempirical electronic structure package, Version 2.9; Max-Planck-Institut für Bioanorganische Chemie: Mülheim (Germany).
(48) Weigend, F.; Ahlrichs, R. Balanced basis sets of split valence, triple zeta valence and quadruple zeta valence quality for H to Rn: design and assessment of accuracy. *Phys. Chem. Chem. Phys.* **2005**, *7*, 3297−3305.
(49) Malkin, V. G.; Malkina, O. L.; Reviakine, R.; Arbuznikov, A. V.; Kaupp, M.; Schimmelpfennig, B.; Malkin, I.; Helgaker, T.; Ruud, K. MAG-ReSpect, Version 1.1; 2003.
(50) Lee, C.; Yang, W.; Parr, R. G. Development of the Colle-Salvetti correlation-energy formula into a functional of the electron density. *Phys. Rev. B* **1988**, *37*, 785−789.
(51) Becke, A. D. Density-functional thermochemistry. III. The role of exact exchange. *J. Chem. Phys.* **1993**, *98*, 5648−5652.
(52) Barone, V. In *Recent advances in density-functional methods*; Chong, D. P., Ed.; World Scientific Publishing: Singapore, 1996; Vol. *1*, pp 287−334.
(53) Daviso, E.; Janssen, G. J.; Alia, A.; Jeschke, G.; Matysik, J.; Tessari, M. A 10000-fold nuclear hyperpolarization of a membrane protein in the liquid phase via a solid-state mechanism. *J. Am. Chem. Soc.* **2011**, *133*, 16754−16757.
(54) Himo, F.; Eriksson, L. A. Theoretical study of model tryptophan radicals and radical cations: comparison with experimental data of DNA photolyase, cytochrome *c* peroxidase, and ribonucleotide reductase. *J. Phys. Chem. B* **1997**, *101*, 9811−9819.
(55) Kobori, Y.; Fuki, M.; Murai, H. Electron spin polarization transfer to the charge-separated state from locally excited triplet configuration: theory and its application to characterization of geometry and electronic coupling in the electron donor−acceptor system. *J. Phys. Chem. B* **2010**, *114*, 14621−14630.
(56) Prakash, S.; Alia; Gast, P.; de Groot, H. J. M.; Jeschke, G.; Matysik, J. Magnetic field dependence of photo-CIDNP MAS NMR on photosynthetic reaction centers of *Rhodobacter sphaeroides* WT. *J. Am. Chem. Soc.* **2005**, *127*, 14290−14298.
(57) Hore, P. J.; Egmond, M. R.; Edzes, H. T.; Kaptein, R. Cross-relaxation effects in the photo-CIDNP spectra of amino acids and proteins. *J. Magn. Reson.* **1982**, *49*, 122−150.
(58) Kay, C. W. M.; Bittl, R.; Bacher, A.; Richter, G.; Weber, S. Unambiguous determination of the g-matrix orientation in a neutral flavin radical by pulsed electron−nuclear double resonance at 94 GHz. *J. Am. Chem. Soc.* **2005**, *127*, 10780−10781.
(59) Schleicher, E.; Kowalczyk, R. M.; Kay, C. W. M.; Hegemann, P.; Bacher, A.; Fischer, M.; Bittl, R.; Richter, G.; Weber, S. On the reaction mechanism of adduct formation in LOV domains of the plant blue-light receptor phototropin. *J. Am. Chem. Soc.* **2004**, *126*, 11067−11076.
(60) Kowalczyk, R. M.; Schleicher, E.; Bittl, R.; Weber, S. The photo-induced triplet of flavins and its protonation states. *J. Am. Chem. Soc.* **2004**, *126*, 11393−11399.
(61) Corchnoy, S. B.; Swartz, T. E.; Lewis, J. W.; Szundi, I.; Briggs, W. R.; Bogomolni, R. A. Intramolecular proton transfers and structural changes during the photocycle of the LOV2 domain of phototropin 1. *J. Biol. Chem.* **2003**, *278*, 724−731.
(62) Kennis, J. T. M.; Crosson, S.; Gauden, M.; van Stokkum, I. H. M.; Moffat, K.; van Grondelle, R. Primary reactions of the LOV2 domain of phototropin, a plant blue-light photoreceptor. *Biochemistry* **2003**, *42*, 3385−3392.
(63) Kottke, T.; Heberle, J.; Hehn, D.; Dick, B.; Hegemann, P. Phot-LOV1: photocycle of a blue-light receptor domain from the green alga *Chlamydomonas reinhardtii*. *Biophys. J.* **2003**, *84*, 1192−1201.
(64) Sato, Y.; Iwata, T.; Tokutomi, S.; Kandori, H. Reactive cysteine is protonated in the triplet excited state of the LOV2 domain in *Adiantum* phytochrome3. *J. Am. Chem. Soc.* **2005**, *127*, 1088−1089.
(65) Alexandre, M. T. A.; Domratcheva, T.; Bonetti, C.; van Wilderen, L. J. G. W.; van Grondelle, R.; Groot, M.-L.; Hellingwerf, K. J.; Kennis, J. T. M. Primary reactions of the LOV2 domain of phototropin studied with ultrafast mid-infrared spectroscopy and quantum chemistry. *Biophys. J.* **2009**, *97*, 227−237.
(66) Thöing, C.; Pfeifer, A.; Kakorin, S.; Kottke, T. Protonated triplet-excited flavin resolved by step-scan FTIR spectroscopy: implications for photosensory LOV domains. *Phys. Chem. Chem. Phys.* **2013**, *15*, 5916−5926.
(67) Nagai, H.; Fukushima, Y.; Okajima, K.; Ikeuchi, M.; Mino, H. Formation of interacting spins on flavosemiquinone and tyrosine radical in photoreaction of a blue light sensor BLUF protein TePixD. *Biochemistry* **2008**, *47*, 12574−12582.
(68) Weber, S.; Schroeder, C.; Kacprzak, S.; Mathes, T.; Kowalczyk, R. M.; Essen, L.-O.; Hegemann, P.; Schleicher, E.; Bittl, R. Light-generated paramagnetic intermediates in BLUF domains. *Photochem. Photobiol.* **2011**, *87*, 574−583.
(69) Kondo, T.; Masuda, S.; Tsutsui, K.; Mino, H. Temperature dependence of relaxation time of a stable radical pair in SyPixD investigated by pulsed EPR. *Chem. Phys. Lett.* **2011**, *501*, 528−533.